Flatness-Based Tracking of an Electromechanical VVT Actuator with Magnetic Flux Sensor

Ryan R. Chladny, *Student Member, IEEE and* Charles R. Koch, *Member, IEEE*

***Abstract*— A flatness-based end controller of an automotive solenoid valve has been demonstrated in both simulation and on an actuator test-bench. The simulation model provides an accurate representation of the real system and allows for the development of control strategies. The simulation results are contrasted with those of an actuator test-bench equipped with 42 volt automotive solenoid valves and a pressure chamber to simulate valve opening with exhaust gas pressures. A flux-based sensor which is suitable for real engine operation is used for position estimation in the soft-landing control.**

***Index Terms*— engines, solenoids, nonlinear control, modeling, magnetic field measurement.**

I. Introduction

Traditional internal combustion engine (ICE) gas exchange valve timing is mechanically fixed by the camshaft. This timing determines when valves open and close, thereby affecting the air-fuel mixture and exhaust flow. Since timing cannot be altered without significant engine modifications, a compromise between low and high engine speed efficiency is assigned [1]. A promising method of improving efficiency is through independent control of gas exchange valve timing. Recently, a confluence of increasing fuel prices, stringent emissions standards, efficient power-electronics and affordable microprocessor and sensor technologies have motivated researchers to investigate the viability of variable valve timing methods. These include electrical motor [2], pneumatic [3], [4], hydraulic [5], [6], and solenoid valve actuators [7], [8]. Many of these approaches cannot provide sufficiently fast, efficient and precise control of cylinder charge during engine transients. Transient cylinder charge control is of particular importance in the transition between combustion modes such as homogeneous charge compression ignition and normal spark ignition. The solenoid actuator used in this work is of a hinged or clapper-type configuration such as those discussed in [10], [11]. An example of a typical hinged solenoid actuator is shown in Figure 1. In the hinged design, the armature equilibrium is balanced between a torsion bar and a linear compression spring. Pole geometry is considered 'U' shaped and made of laminated steel for eddy current suppression.

This work was supported in part by the Natural Sciences and Engineering Research Council of Canada, under Research Grant number 249553-02

The authors would like to thank DaimlerChrysler for the donation of the cylinder head and solenoid valve actuators.

R.R. Chladny and C.R. Koch are with the Department of Mechanical Engineering, University of Alberta (e-mail: rchladny@ualberta.ca; bob.koch@ualberta.ca).

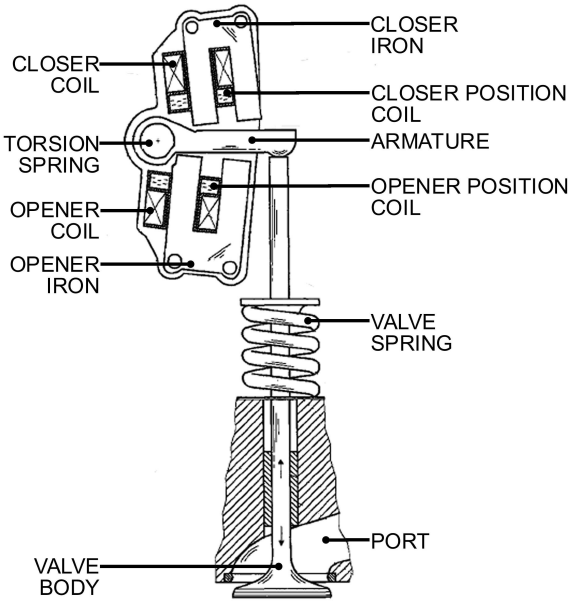

Fig. 1. Hinged electromagnetic gas exchange valve actuator [9]

II. Plant Derivation

A. Magnetic and Electric Subsystems

As a means of providing a more accurate inductance model, magnetic material saturation is considered. Saturation effects will be present at high magnetomotive force (MMF) values, particularly at small armature/pole face air gaps and/or high current excitation [12]. Landing control is expected to be executed while the system is at such conditions.

The following function is intended to approximate the flux linkage response with magnetic material saturation as in [13]:

$$\lambda(x,i) = \psi(1 - e^{-ig(x)}), \tag{1}$$

with,

$$g(x) = \frac{\beta}{\kappa - x} + \alpha. \tag{2}$$

where x represents the 8mm valve stroke, $x\epsilon[-4.00\ 4.00]$ mm and i is the coil current. The parameters ψ, β, κ and α are identified using a nonlinear least squares fit to results from a two-dimensional FEA model as a method of characterizing actuator performance as described in [12]. ANSYS was used for static and transient FEA simulations and the MATLAB function `nlinfit.m` is used for finding least squares parameter estimates.

The electrical domain can be represented by an RL circuit described by Faraday's law of induction and the following KVL equation:

$$v = iR + \frac{d\lambda(i,x)}{dt}, \tag{3}$$

with applied voltage, v, coil current, i, and $\lambda(i,x)$ representing the magnetic flux linkage of the electromagnet. In addition, R, represents the total resistance of the coil winding. The KVL relation may be expressed in state space form by taking current, i, as a state, and input, u, as $u = v - iR$ to yield:

$$\frac{di}{dt} = \frac{1}{g(x)}\left(\frac{e^{g(x)i}u}{\psi} - ig'(x)\dot{x}\right) \tag{4}$$

B. Mechanical Subsystem

The co-energy, W_c, principal [14] is used with respect to the nonlinear inductance model described in (1) to develop a relationship between magnetic force, F_m, armature position, x and current, i,

$$\begin{aligned} F_m(x,i) &= \frac{\partial W_c(x,i)}{\partial x} \\ &= \frac{\psi g'(x)}{g^2(x)}\left(1 - (1 + ig(x))e^{-g(x)i}\right). \end{aligned} \tag{5}$$

Applying Newton's second law, valve motion as a function of magnetic force, spring/torsion bar force and viscous damping is derived:

$$\ddot{x} = -\frac{1}{m}\left(\dot{x}b + xk - F_v + F_g - \frac{\ell_m}{\ell_v}F_m(x,i)\right) \tag{6}$$

where:

- m is the effective system mass
- ℓ_v is the radial distance from the armature pivot point to where the longitudinal armature and valve axes intersect
- ℓ_m is the radial distance from the armature pivot point to where the resultant magnetic force acts on the armature
- b the effective system damping coefficient
- k is the valve spring constant
- F_v is the valve spring pre-load
- F_g is the gas force acting upon the valve
- $F_{m,j} = -F_{m,o}, F_{m,c}$ is the magnetic force on the armature, with $j = o, c$ to indicate the opener or closer magnet respectively

The valve and armature are considered to be rigidly coupled. Sufficiently small angles are assumed such that $\sin\theta \sim \theta$, since θ is limited to $\pm 6.075^o$. In simulation, armature impacts are modeled simply by setting acceleration and velocity to zero when the armature reaches the stroke bounds. External forces such as those caused by gravity, engine and vehicle dynamics are considered negligible.

III. Flatness-Based Voltage Control

A wide variety of control algorithms have been proposed for the soft-seating tracking problem. They include classical linearized model control (about an equilibrium point) [15], proportional integral (PI) [16], [17], linear quadratic regulator (LRQ) [18], full state feedback linearization [19], extremum seeking [20], sliding mode [21] and flatness-based control [22], [23], [24]. Although many of these control schemes are able to attain seating velocities of 0.1m/s or less, they often make use of impractical operating conditions such as the use of external in-cylinder and/or expensive feedback sensors, voltages exceeding 100V or transition times exceeding 5ms. The landing controller proposed in this work uses a flatness-based landing controller as described in [25], [26], [27], [28] to achieve exponentially convergent armature position tracking to a predetermined trajectory. Static state-feedback voltage control is obtained by defining position, x, as a flat output, y. Voltage is related to the third time derivative of y as follows:

$$\begin{aligned} y &= x \\ \dot{y} &= \dot{x} \\ \ddot{y} &= \ddot{x} = -\frac{1}{m}\left(\dot{y}b + yk - F_v + F_g - \frac{\ell_m}{\ell_v}F_m(y,i)\right) \\ y^{(3)} &= -\frac{1}{m}\left(\ddot{y}b + \dot{y}k + \dot{F}_g - \frac{\ell_m}{\ell_v}\dot{F}_m(y,i)\right), \end{aligned} \tag{7}$$

where,

$$\begin{aligned} \dot{F}_m(y,i) =& 2\dot{y}F_m(y,i)\left(\frac{1}{(\kappa - y)} - \frac{g'(y)}{g(y)}\right) \\ &+ \frac{ig'(y)}{g(y)}(v - iR). \end{aligned} \tag{8}$$

Solving (8) for input voltage, v yields:

$$\begin{aligned} v =& \frac{\ell_v g(y)}{\ell_m i g'(y)}\left(\ddot{y}b + \dot{y}(k + 2F_m(y,i)(\frac{g'(y)}{g(y)}\right. \\ &\left. - \frac{1}{(\kappa - y)}) + y^{(3)}m\right) + iR. \end{aligned} \tag{9}$$

The singularity at $i = 0$ is avoided through ensuring a non-zero bias current and appropriate reference trajectory design as discussed in Section IV. Non-zero current is also a requirement for flux-based position reconstruction as described in Section V. From (9) it is apparent that the state $(i, x, \dot{x})$ and input, v, may be expressed as a finite number of time derivatives of the output, y. Therefore the system satisfies the flatness definition and the tracking methods outlined in work such as [29], [30] are applicable. Defining tracking error as $\tilde{y} = y - y_d$, linear error dynamics are defined by

$$y^{(3)} = -k_1\tilde{y} - k_2\dot{\tilde{y}} - k_3\ddot{\tilde{y}} + y_d^{(3)} \tag{10}$$

Substitution of (10) into (9) results in an expression for closed loop voltage control. Exponential tracking of y to y_d will be achieved provided that the gains k_i are positive and chosen appropriately.

IV. Reference Trajectory Design

Optimal reference trajectories are sought subject to physical, practical and desired end condition constraints. The MATLAB optimization routine `fmincon.m` is used to optimize spline coefficients which parameterize a fifth order trajectory set. A cost function is used to minimize electromagnetic force. A detailed description of the method used is provided in [23] for a linear motion actuator. The constraints imposed are

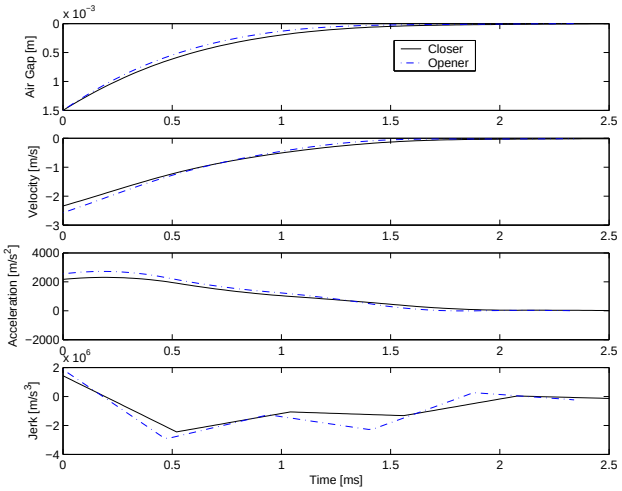

Fig. 2. Optimized reference trajectories for the hinged actuator with nonlinear induction model

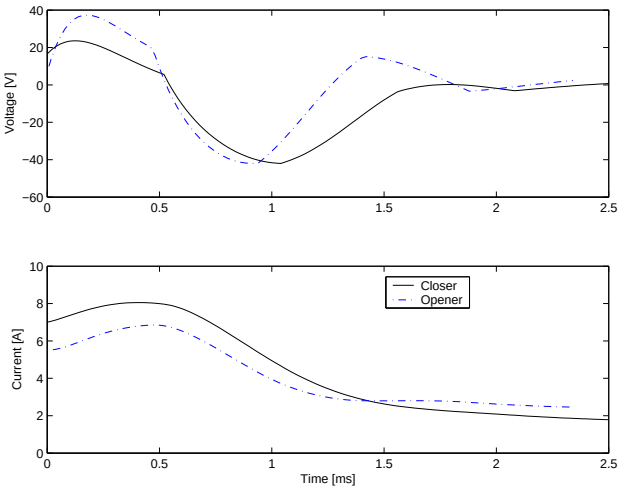

Fig. 3. Coil input corresponding to the optimized reference trajectories for the hinged actuator and nonlinear induction model

listed in Table I where t_o and t_f are the times when the landing controller are respectively engaged and disengaged. Figure 2 illustrates a set of reference trajectories starting from a set of simulated initial conditions and Figure 3 represents the corresponding voltage and current input. Note that for the purposes of comparison, the opener and closer reference trajectories are shown relative to their respective magnet pole faces.

V. Flux-Based Position Feedback

Due to the low-impact speed requirement of the valve and significant combustion pressure fluctuations feedback control is required. Thus, a means of accurately sensing armature or valve position is required for the feedback control. Efforts have been made to develop alternative cost effective sensors or sensing methods as alternatives to established, although more expensive methods [31]. These include the flux-based coil type [11], [32], [33], [34], [35], observer-based [36], [21] and self-inductive [37], [38] schemes. The latter cases are sensitive

TABLE I

Reference Trajectory Constraints

Position (Air Gap)	Velocity
$y_d(t_o)$ = 1.50 mm $y_d(t_f)$ = 0.00 mm	$\dot{y}_d(t_0) = \dot{y}_o$ m/s $\dot{y}_d(t_f) \leq 0.1$ m/s $\dot{y}_d(t) \geq 0, t_o < t < t_f$
Acceleration	**Voltage & Current**
$\ddot{y}_d(t_o) = -1/m\,(\dot{y}_d(t_o)b + y_d(t_o)k - F_v$ $-\ell_m F_m(y_d(t_0), i(t_o))/\ell_v)$ m/s^2 $\ddot{y}_d(t_f) = 0$m/s^2 $\ddot{y}_d(t) > -1/m\,(\dot{y}_d(t_o)b + y_d(t_o)k - F_v$ $+F_g(t_o))\,, t_o < t < t_f$	$v(t) \leq 42$V, $t_o \leq t \leq t_f$ $i(t_o) = i_o$ A

to initial conditions, suspect to noise disturbances and thus perhaps of limited practical use.

The flux-based coil method of state estimation uses the relationship between magnetic flux, inductance and coil excitation. In the case of devices with variable air gaps such as solenoid actuators, the inductance is highly dependant on armature position, and in the case of the hinged actuator, valve position. Thus valve position may be predicted using measurements of the coil current and path flux. Current is already measured with a hall-effect device and flux may be measured with a secondary coil and analog integration circuit. The hinged actuator accomplishes this by including a secondary coil concentric to the excitation coil. Thus, any time-varying magnetic field produced by the excitation coil will induce an electromotive force (EMF) as predicted by Faraday's law of mutual inductance. Assuming the secondary coil is measured with high impedance circuitry, resistance of the flux loop is negligible and the induced voltage due to a change in excitation current or flux may be expressed as:

$$v_{fc} = N_{fc}\frac{d\phi(i,x)}{dt} = \frac{N_{fc}}{N_{ec}}\frac{d\lambda(i,x)}{dt}, \tag{11}$$

where v_{fc} is the induced voltage in the flux coil, $\frac{d\phi}{dt}$ is the flux induced potential and N_{fc} and N_{ec} are the respective number of turns for the flux coil and excitation coil. In practice, the induced voltage is integrated (analog) and sampled. Thus, the integrated result may be expressed as:

$$\lambda = N_{ec}(\phi_o + \frac{\int v_{fc}dt}{N_{fc}}), \tag{12}$$

where ϕ_o is the initial flux condition prior to integration. Using the derived flux model in (1), a relationship between current, flux and armature position is expected to be of the form:

$$x = \frac{\beta i}{\alpha i + ln(1 - N_{ec}/\psi(\phi_o + \int v_{fc}dt/N_{fc}))} + \kappa \tag{13}$$

A consequence of this relationship is that a position measurement can only be observed with a non-zero current being applied. This restriction is also imposed in order to satisfy controllability conditions (Section III). This method of position reconstruction is similar to [11], in which two functions are used to relate reluctance and excitation to air gap. Our efforts have shown that improved accuracy over Equation (13) is achieved through use of a numerical look-up table with FEA results relating flux and current to position. Velocity is

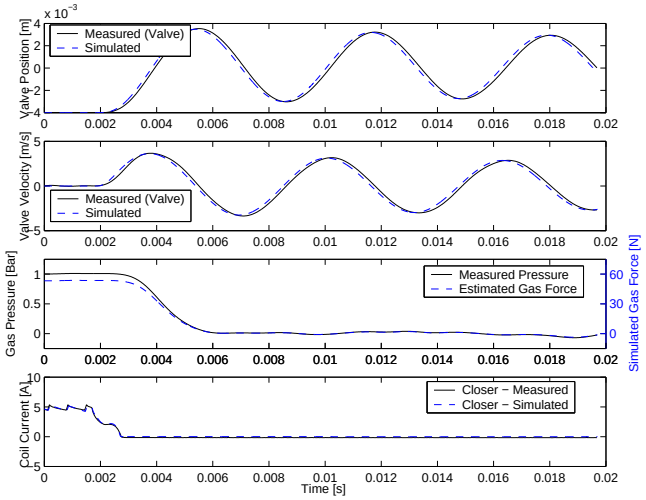

Fig. 4. Simulated and experimental position, velocity, pressure and release current during a free opening at 1Bar blowdown pressure

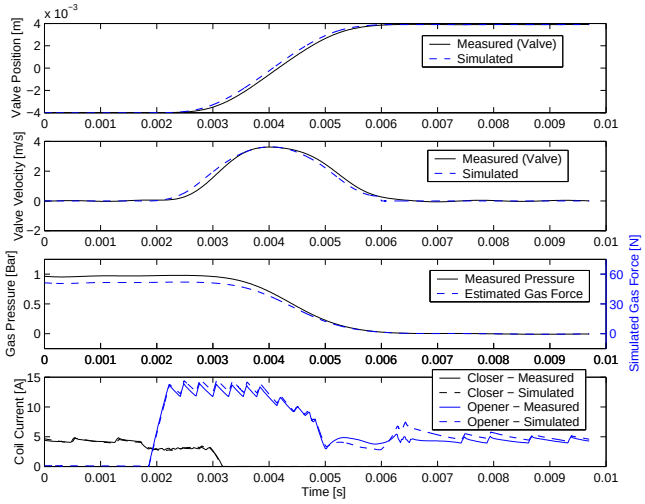

Fig. 5. Simulated and experimental valve opening, 1Bar blowdown pressure

estimated using the calculated position and an 'alpha-beta' Kalman filter.

VI. Dynamic Simulation

Prior to test-bench implementation, a model of the complete actuator system was developed using the MATLAB Simulink environment and acquired FEA data. The model accounts for bridge drive circuits, mechanical and electromagnetic response. Recently the model was extended to incorporate gas foces as a means to evaluate feedforward requirements under a variety of blowdown pressures. The model was then validated through comparison to increasingly involved test-bench experiments using the apparatus described in Section VII. Figures 4 and 5 contrast the simulated and experimental results of pressurized release and opening instances respectively. In these cases, the pressure trace and digital outputs from the dSPACE controller were recorded and used as the model input (open-loop simulation). Gas force was estimated to be equal to valve area times cavity pressure. However, this is likely conservative as the actual force is likely less due to portions of the flow stagnating on the rear of the valve [39]. The simulation results suggest reasonable agreement given the simple gas force model, particularly when the main advantage of having full valve cycle modeling capability is in the feedforward design. Specifically, a maximum of 1.5% displacement and velocity peak error among the various simulations was observed. The primary discrepancy is due to a 0.25ms delay (maximum) between the measured and simulated results. This may be due to a delay in reference position (laser sensor output) and sampling. The model is also capable of simulating landing control as shown in Figure 6. In this case a tuned PI controller and the flatness-based voltage control are contrasted with equivalent experimental conditions. Again reasonable agreement between the flatness-based simulation and experiment is achieved. Maximum velocity error of 0.1m/s occurs at impact. However, the modeling error is more difficult to quantify in the closed loop case due a discrepancy in the experimental and simulated PWM voltage commands. In these

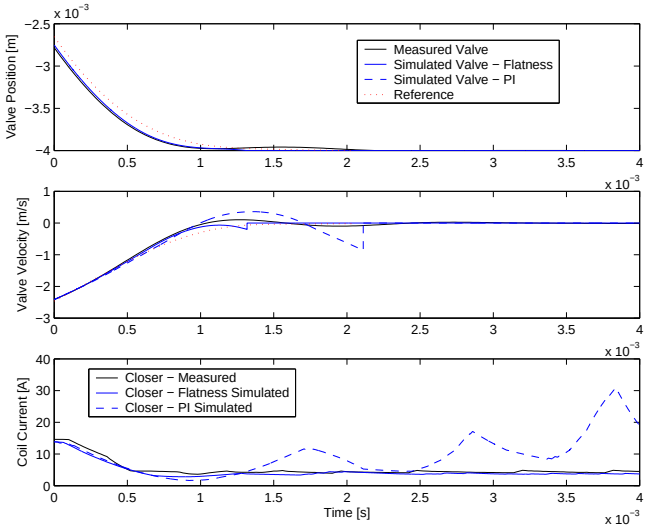

Fig. 6. Flatness, PI and experimental valve closing via flux position estimation

simulations, as in hardware, the closed loop control voltage output is converted into bridge switching logic signals (consisting of a PWM and TTL signal) to approximate the desired voltage. Overall, the simulations indicate the flatness-based control offers superior performance over PI algorithms with respect to settling time, impact velocity, energy consumption and robustness, particularly when initial conditions deviate in excess of 10% of the ideal initial reference conditions.

VII. Experimental Setup

After qualifying the FEA results using a similar procedure and apparatus described in [40] for the hinged actuator, a test-bench setup was designed and fabricated that utilizes a complete single cylinder engine head. By making use of an actual engine head, realistic engine operating conditions can be emulated in order to evaluate various control strategies and sensing techniques. Figure 7 illustrates the test-bench configuration. The cylinder head is supported through three

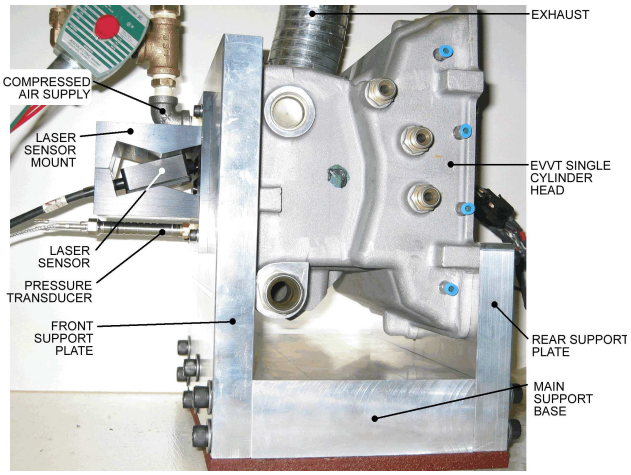

Fig. 7. Single cylinder head test-bench setup

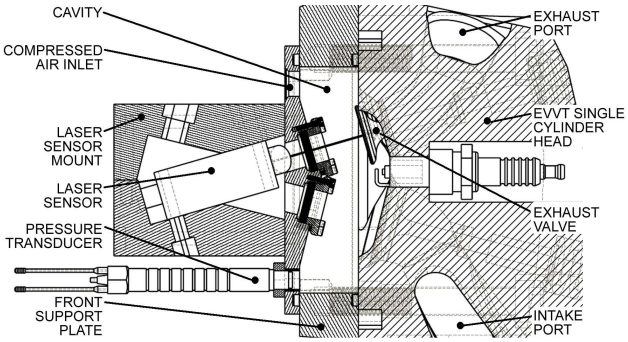

Fig. 8. Sectional view of cylinder head test-bench cavity

aluminum plates bolted to a steel sub-frame (not shown). The front support plate has a centrally located cylindrical hole with a diameter corresponding to the engine bore. The cavity is tunable in order to produce realistic exhaust pressure transients. Compressed air from the building supply is used to pressurize the cavity. Pressure is controlled electronically between 0 and 6 bar via dSPACE 1103 hardware, a Wilkerson ER1 electromechanical pressure regulator, ASCO 104R three-way solenoid valve, Kistler 6043A60 pressure transducer and Sundstrand 507 charge amplifier. Pressure pulsations are damped by passing regulated air through a 0.041m^3 (11 gal) tank. A Micro-Epsilon LD162710 laser transducer monitors exhaust valve position and is not used for control. Figure 8 represents a cross-section of the air cavity with laser and pressure sensor configuration. Electric power is supplied at 42V to the actuator by a Sorensen DCS 80-37 3kW programable supply via custom designed H-bridge power electronics. All other hardware accessories such as custom opto-isolation and current overload protection circuits are powered through an HP 6236B triple output supply. All actuator control is performed using dSPACE 1103 hardware. Flux signals estimate valve position via custom electronics and software which are used in the feedback control.

VIII. Experimental Tracking Performance

Upon fabrication and assembly of the hinged actuator test-bench, landing control was evaluated over a variety of operating conditions. To ensure suitable landing control initial conditions and to overcome gas forces, an open loop feedforward current control scheme was implemented for both the opener and closer magnets. The disturbance pressure, which simulates exhaust valve combustion pressure, was regulated within 0.1 bar of a given pressure setpoint. Figure 9 demonstrates typical landing performance (opening and closing) over a pressure range of 0.25 to 4.5 bar using the flux-based position and velocity estimation. It was found that landing velocities of $\leq$ 0.1m/s were consistently attainable. Figure 10 illustrates similar performance is attainable at higher test-bench speeds as well. However, at speeds greater than 3000rpm, exhaust pressures are limited to approximately 1 bar due to compressed air supply restriction on the testbench.

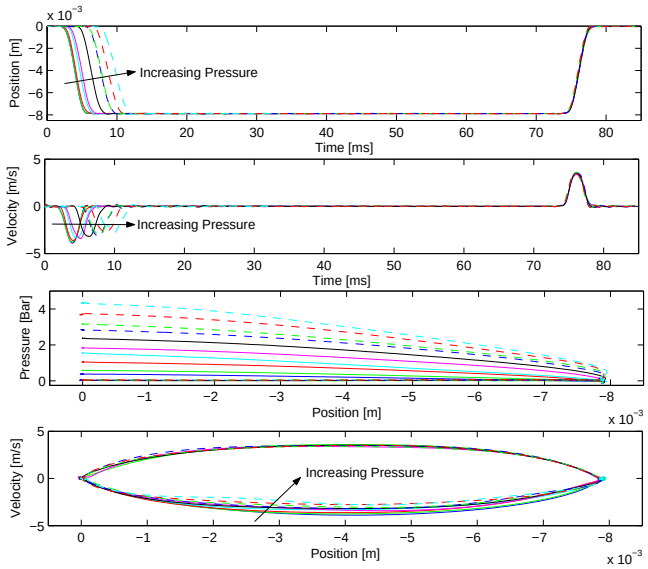

Fig. 9. Full cycle plots over a 0.25 to 4.5 bar pressure range, 250rpm

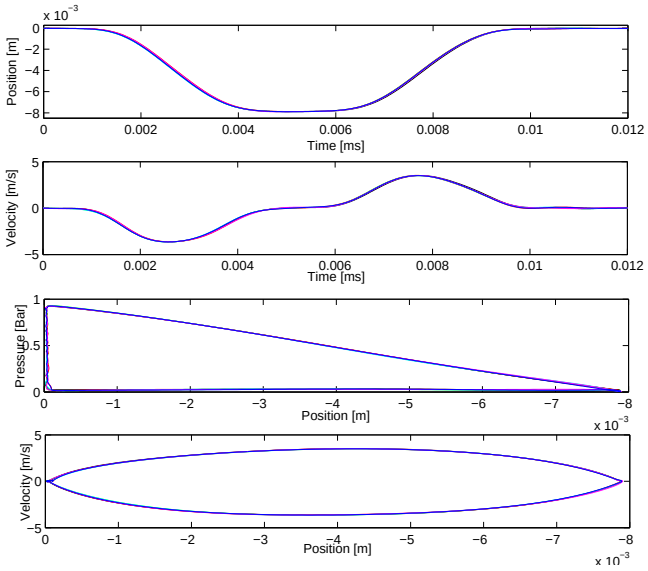

Fig. 10. Flatness voltage landing control via flux feedback - 3500rpm, 1 bar blowdown, 6 cycles

IX. Conclusion

Simulated and experimental performance of a flatness-based landing controller using a flux-based position reconstruction method has been contrasted. The developed actuator simulation has proven to be sufficiently accurate to both develop and test suitable control strategies. A method of experimental testing of a hinged actuator has been outlined. This apparatus provides an excellent way to validate the simulation and provides a realistic proving ground for control development prior to engine implementation. By tuning an open loop feedforward controller, valve seating velocities ≤ 0.1m/s with up to 4.5 bar simulated combustion pressure disturbance on the test-bench are attainable. Further work is being pursued with respect to online disturbance identification techniques in simulation and test-bench hardware in preparation for single cylinder engine implementation.

References

[1] M. Schechter and M. Levin, "Camless engine," *SAE paper 960581*, 1996.

[2] R. Henry, "Single-cylinder engine tests of a motor-driven variable-valve actuator," *SAE paper 2001-01-0241*, 2001.

[3] W. Richeson and F. Erickson, "Pneumatic actuator with permanent magnet control valve latching," *U.S. Patent No. 4,852,528*, 1989.

[4] L. Gould, W. Richeson, and F. Erickson, "Performance evaluation of a camless engine using valve actuators with programmable timing," *SAE paper 910450*, 1991.

[5] J. Allen and D. Law, "Production electro-hydraulic variable valve-train for a new generation of I.C. engines," *SAE paper 2002-01-1109*, 2002.

[6] S. Barros da Cunha, J. Hedrick, and A. Pisano, "Variable valve timing by means of a hydraulic actuation," *SAE paper 2000-01-1220*, 2000.

[7] M. Pischinger, W. Salber, F. van der Staay, H. Baumgarten, and H. Kemper, "Benefits of the electromechanical valve train in vehicle operation," *SAE paper 2000-01-1223*, 2000.

[8] B. Lequesne, "Fast acting, long-stroke solenoids with two springs," *IEEE Trans. Ind. Applicat.*, vol. 26, pp. 848–856, 1990.

[9] T. Stolk and A. Gaisberg, "Elektromagnetischer aktuator," *German Patent Application DE 10025491 A1*, 2001.

[10] Y. Kawase, H. Kikuchi, and S. Ito, "3-D nonlinear transient analysis of dynamic behavior of the clapper type DC magnet," *IEEE Trans. Magn.*, vol. 27, no. 5, pp. 4238–4241, 1991.

[11] M. Montanari, F. Ronchi, C. Rossi, and A. Tonielli, "Control of a camless engine electromechanical actuator: Position reconstruction and dynamic performance analysis," *IEEE Trans. Ind. Electron.*, vol. 51, pp. 299–311, 2004.

[12] R. Chladny, C. Koch, and A. Lynch, "Modeling automotive gas-exchange solenoid valve actuators," *IEEE Trans. Magn.*, vol. 41, pp. 1155–1162, 2005.

[13] Ilic'-Spong and M., R. Marino and S. Peresada and D. Taylor, "Feedback linearizing control of switched reluctance motors," *IEEE Trans. Auto. Contr.*, vol. 32, no. 5, pp. 371–379, 1987.

[14] H. Woodson and J. Melcher, *Electromechanical Dynamics Part I: Discrete Systems*. John Wiley & Sons, 1968.

[15] R. Konrad, "Verfahren zur Bewegungssteuerung für einen ankers eines elektromagnetishen Aktuators," *German Pat. Appl. 19834548 A1*, 1998.

[16] C. Tai and T. Tsao, "Quiet seating control design of an electromagnetic engine valve actuator," *Proc. 2001 ASME International Mechanical Engineering Congress and Exposition*, 2001.

[17] A. Stubbs, "Modeling and controller design of an electromagnetic engine valve," *Master's thesis, University of Illinois at Urbana-Champaign*, 2000.

[18] C. Tai and T. Tsao, "Control of an elctromechanical actuator for camless engines," *Proc. 2003 American Control Conference*, 2003.

[19] I. Haskara, V. Kokotovic, and L. Mianzo, "Control of an elctromechanical valve actuator for a camless engine," *International Journal of Robust and Nonlinear Control*, vol. 14, pp. 561–579, 2004.

[20] K. Peterson and A. Stefanopoulou, "Extremum seeking control for soft landing of an electromechanical valve actuator," *Automatica*, 2004.

[21] P. Eyabi, "Modeling and sensorless control of solenoid actuators," *Ph.D. thesis, Dept. Mechanical Engineering, Ohio State University*, 2003.

[22] S. Chung, "Flatness-based voltage end control of a gas exchange solenoid actuator for IC engines," *M.Sc. thesis, Dept. Mechanical Engineering, University of Alberta*, 2005.

[23] C. Koch, A. Lynch, and S. Chung, "Flatness-based automotive solenoid valve control," *6th IFAC Symp. Nonlin. Contr. Systems (NOLCOS)*, pp. 1091–1096, 2004.

[24] P. Mercorelli, K. Lehmann, and S. Liu, "Robust flatness based control of an electromagnetic linear actuator using adaptive PID controller," *Proceedings of the IEEE Decision and Control Conference*, pp. 3790–3795, 2003.

[25] J. Lévine, "On flatness necessary and sufficient conditions," *6th IFAC Symp. Nonlin. Contr. Systems (NOLCOS)*, pp. 125–130, 2004.

[26] J. Löewis, "Flachheitsbasierte Trajektorienfolgeregelung elektromechanischer Systeme," Ph.D. dissertation, TU-Dresden, 2002.

[27] F. Woittennek, "Untersuching flachheitsbasierter nichtlinearer Regler für magnetgelagerte Wellen," Master's thesis, TU-Dresden, Germany, 1999.

[28] J. Lévine, J. Lottin, and J.-C. Ponsart, "A nonlinear approach to the control of magnetic bearings," *IEEE Trans. Contr. Syst. Technol.*, vol. 4, no. 5, pp. 524–544, Sep. 1996.

[29] M. Fliess, J. Lévine, P. Martin, and P. Rouchon, "A Lie-Bäcklund approach to equivalence and flatness of nonlinear systems," *IEEE Trans. Auto. Contr.*, vol. 44, no. 5, pp. 922–937, 1999.

[30] ——, "Flatness and defect of non-linear systems: Introductory theory and examples," *Int. J. Control*, vol. 61, no. 6, pp. 1327–1361, 1995.

[31] R. Chladny and C. Koch, "A Magnetic Flux-Based Position Sensor for Control of an Electromechanical VVT Actuator," *To be published in the 2006 American Control Conference proceedings*, September 2006.

[32] A. Scacchioli, "Hybrid regulation of electromagnetic valves in automotive systems," *Ph.D. thesis, Dept. of Electrical Engineering, University of LAquila*, 2005.

[33] C. Rossi and T. Alberto, "Method and device for estimating the position of an actuator body in an electromagnetic actuator to control a valve of an engine," *Magneti Marelli European Patent Application EP 1152129 A1*, 2001.

[34] C. Rossi and A. Tonielli, "Method and device for estimating the position of an actuator body in an electromagnetic actuator to control a valve of an engine," *European Patent Application EP 1152129 A1*, 2001.

[35] T. Roschke and M. Bielau, "Verfahren zur modellbasierten Messung und Regelung von Bewegungen an elektromagnetischen Aktoren," *Technische Universitaet Dresden German Patent Application DE 19544207 A1*, 1995.

[36] A. Lynch, C. Koch, and R. Chladny, "Nonlinear observer design for sensorless electromagnetic actuators," *3rd International Conference on Dynamics of Continuous, Discrete and Impulsive Systems, May 2003*, 2003.

[37] S. Butzmann, J. Melbert, and A. Koch, "Sensorless control of electromagnetic actuators for variable valve train," *SAE paper 2000-01-1225*, 2000.

[38] D. Takashi and M. Iwao, "Valve drive device for internal combustion engine and initial position setting method for valve element," *Japan Patent Application JP 0224624*, 1995.

[39] C. Schernus, F. van der Staay, H. Janssen, J. Neumeister, B. Vogt, L. Donce, I. Estlimbaum, E. Nicole, and C. Maerky, "Modeling of exhaust valve opening in a camless engine," *SAE paper 2002-01-0376*, 2002.

[40] R. Chladny, "Modeling and simulation of automotive gas exchange valve solenoid actuators," *M.Sc. thesis, Dept. Mechanical Engineering, University of Alberta*, 2003.